

# Segmentation of laminar shape objects obtained from TEM tomography for a quantitative microstructural analysis

*Iturrondobeitia, Mainer; Ibarretxe, Julen; Fernandez Martinez, Roberto; Jimbert, Pello; Okariz, Ana and Guraya, Teresa*  
*eMERG (University of the Basque Country-EHU-UPV, Spain)*  
*mainer.iturrondobeitia@ehu.eus*

## Keywords

Tomography, segmentation, microstructure, polymer/clay nanocomposites.

## Introduction

The physicochemical properties of polymer nanocomposites, such as polymer/clay, are dependent on the properties of the polymer and filler, the filler or reinforcement dimensionality, dispersion and orientation, and the nature of the interface between filler and matrix. Thus, the final properties of a composite are highly dependent on its morphology on different length scales. Hence, thoroughly characterizing the morphology of those materials can lead to a better understanding of the behaviour of the final product and to improved design tools.

The objective of performing electron tomography (ET) on PLA/clay samples is to characterize their 3D microstructure, by obtaining the dispersion, distribution and orientation of the laminar shape clays, as well as morphological details, such as their specific area or shape factor (figure 1, bottom).

The accuracy of quantitative ET relies, among other factors, on the quality of the 3D reconstruction, which in turn depends on the angular tilt range which determines the missing wedge and as consequence the elongation effect. Other factors affecting the accuracy of the results are the angular increments used for the acquisition, the accuracy of image alignment of the tilt series, the reconstruction algorithm used and the segmentation of the objects<sup>i,ii</sup>. In this study we focus on the segmentation step, which is essential in order to quantitatively analyze the reconstructed volume. Actually, the tedious manual segmentation still remains as the prevalent method of choice.

In this regard, the main purpose of this study is the formulation of a simple, efficient and semi-automated methodology to perform the segmentation. The segmentation threshold is optimized taking into account the rate of variation in the measured dimensions of the segmented objects as a function of the grey level used as threshold. For this purpose a set of fictitious laminar objects is used.

## Materials and Methods

As shown in figure 1 (top), a fictitious volume containing 3 laminar shape objects, each placed in a different position and orientation and accounting in total for a 1.2 vol % of the study volume, was created. From that fictitious volume, a tilted series was generated using the Radon transform<sup>iii</sup> to simulate the corresponding set of TEM tilted images. Thus, the artifacts and errors inherent to the experimentally acquired tilt series were avoided and the derived artifacts in the subsequent ET reconstruction eliminated. The tilt images were simulated every 2 ° over an angular range of  $\pm 70$  °, in order to mimic the conditions used for the experimental tilt series of the actual nanocomposites (figure 1, top). Moreover, the images that form the simulated tilted series do not require any

alignment. The series was reconstructed using the weighted back projection (WBP) algorithm using the IMOD software<sup>iv</sup>. The segmentation of the reconstructions was carried out using Amira<sup>v</sup>. The proposed segmentation methodology is based on the threshold segmentation. Also, it is based on a criterion derived from the variation of the dimensions of the segmented objects. In short, the methodology consists of:

- a) Selection of the range of grey levels that will be applied. The lower and upper limit grey values should result in reconstructed volumes that are almost empty or completely full of objects of interest.
- b) Definition of a given number of evenly distributed grey level values within the dynamic range selected in the previous step. In this work the selected number of thresholds was ten, but the number of used thresholds can be varied if required.
- c) Segmentation by creating isosurfaces for each threshold selected in the previous step.
- d) Projection of the segmented volumes onto the OXY plane, resulting in ten 2D 0 ° tilt projection images in our case of study.
- e) Measurement of the variation in the dimensions of the objects resulting from consecutive thresholds, by means of the cross-correlation factor (R) computed for the 0 ° tilt projections
- f) Selection of the best segmentation threshold for which the correlation with the previous and next threshold values is maximum.

For the fictitious volume, the exact volume of the objects, as well as their position and orientation are known. Despite the existence of the elongation effect inherent to the reconstruction algorithms, the volume of the objects was used as the main criteria to validate the methodology proposed herein. The accuracy of the morphological measurements was also calculated. As illustrated in Figure 1, bottom, for this purpose the length and the thickness of the objects (measured as the minimum and maximum ferets), the area, the volume and their orientation was measured for both, real and reconstructed fictitious volumes and then compared. The orientation was defined by the Theta ( $\theta$ ) and Phi ( $\varphi$ ) angles described in figure 1, bottom.

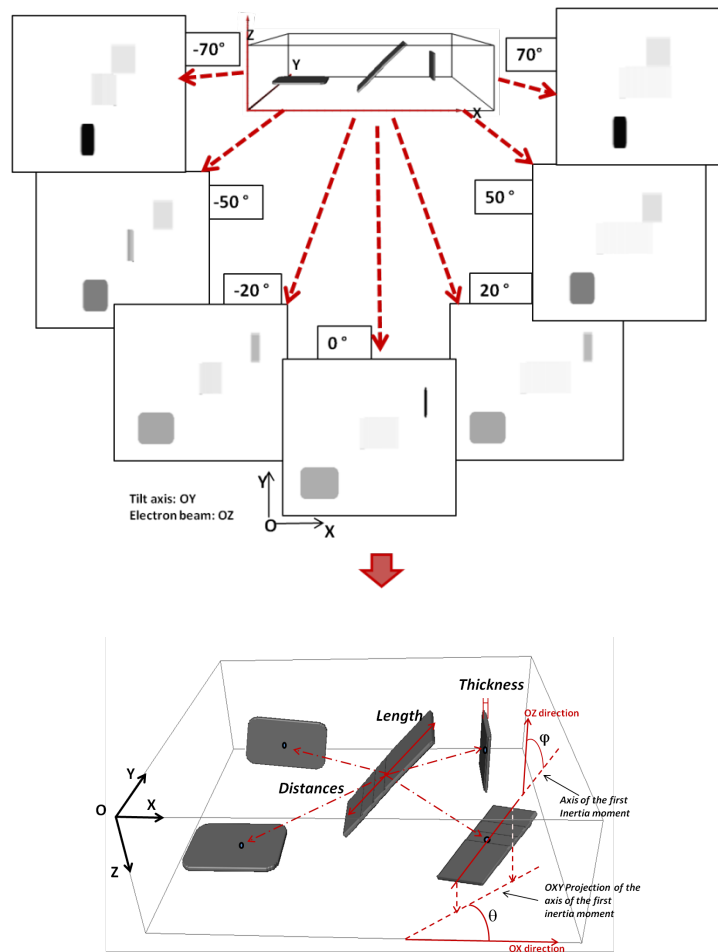


Figure 1. Illustration of the created fictitious objects and volume and the ET reconstruction procedure (top) and a possible quantification of the microstructural descriptors for a 3D reconstruction of lamellar shape objects (bottom).

## Results and Discussion

As shown in figure 2, the highest R values between a projection and its two adjacent projections happens for segmentation number 4. The volume measured for the segmented objects, 1.3 vol. % is very close to the real 1.2 vol. %. Consequently, considering both criteria segmentation number 4 can be appointed as the optimum for the case of the fictitious volume.

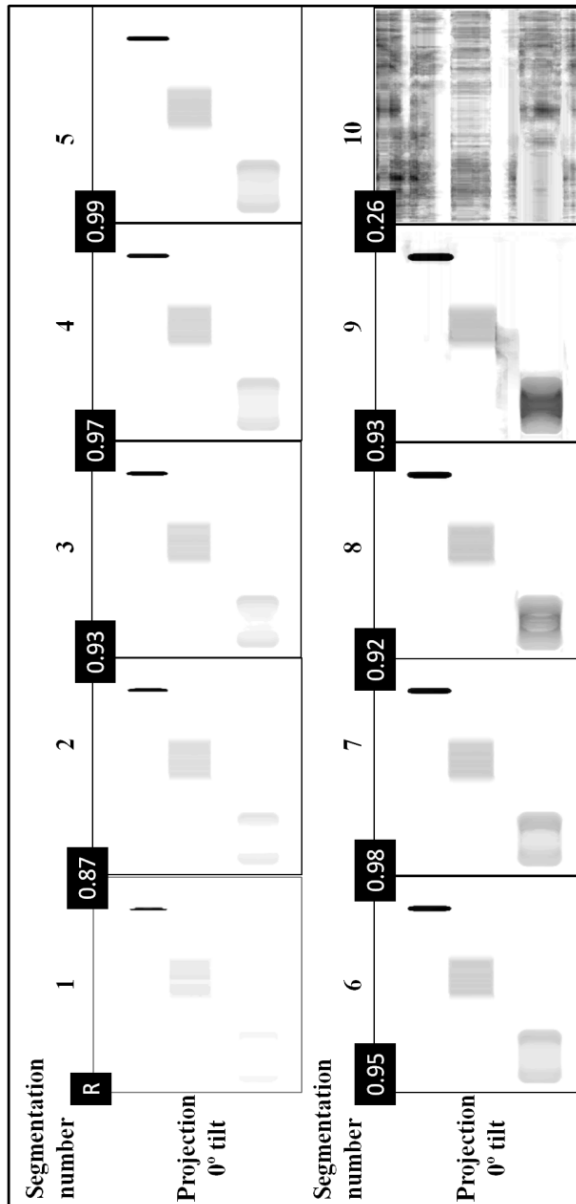


Figure 2.  $0^\circ$  tilt projections of the ten segmentations performed on the tomographic reconstruction of the fictitious volume and the corresponding cross-correlation factors (R) calculated for consecutive projections.

The morphological descriptors shown in table 1 were quantified and their accuracy was assessed by comparing the values obtained for the original fictitious volume and those measured from the segmentation of the reconstructed fictitious volume performed here.

Table 1. Comparison between the parameters quantified for the original fictitious objects and the reconstructed and segmented ones. Orientation: d=diagonal object; v: vertical object; h: horizontal object;  $d$ : thickness;  $L$ : length;  $A'$ : surface area of each object;  $V$ : volume of each of object; Theta: angle between the projection of the first inertia axis and the OX axis; Phi: angle between the direction of the first inertia axis and the OZ axis.

Orientation	$d$	$L$	$A'$	$V$	Theta	Phi
$n$	(pixel)	(pixel)	(pixel <sup>2</sup> )	(pixel <sup>3</sup> )	( $^\circ$ )	( $^\circ$ )

<b>Original fictitious volume</b>	<b>d</b>	7	112	11964	24863	0	45
	<b>v</b>	5	51	5358	11850	0	0
	<b>h</b>	4	73	7772	15140	0	90
<b>Segmented fictitious volume</b>	<b>d</b>	9	109	10964	26950	1	43
	<b>v</b>	8	53	5800	15771	0	0
	<b>h</b>	10	74	8073	21423	0.2	89.8

## Conclusion

An automated, simple and objective segmentation procedure for ET has been proposed and validated. Overall, there is a very high agreement between the measurements for the original objects and the reconstructed and segmented ones. The main discrepancies are observed for those magnitudes that are influenced by the elongation along the OZ axis due to the missing wedge effect, such as the volume or the dimension of the object in the OZ direction. As expected, the surface area values are quantified more precisely than the volumes, which is fortunate due to the higher relevance of the surface area to determine the reinforcing effect of the laminar shape objects, such as the clays.

## References

- Wang, X.Y.; Lockwood, R.; Malac, M.; Furukawa, H.; Li, P.; Meldrum, A. (2012) 'Reconstruction and visualization of nanoparticle composites by transmission electron tomography' *Ultramicroscopy*, V.113. pp. 96-105.
- Fernandez, J.J. (2012) 'Computational methods for electron tomography' *Micron*, V. 43. pp. 1010-1030.
- Radon, J.; Ber, V.K. (1917) *Sach Ges Wiss Leipzig Math Phys Kl*, V. 68. pp. 262.
- Kremer, J.R.; Mastrorarde, D.N.; McIntosh, J.R. (1996) '[Computer visualization of three-dimensional image data using IMOD](#)' *J. Struct. Biol.* V. 116. pp.71-76.

